JOURNAL OF THEORETICAL AND APPLIED MECHANICS
42, 1, pp. 83-93, Warsaw 2004

INFLUENCE OF THE MEAN LOADING ON FATIGUE CRACK GROWTH RATE AND LIFE UNDER BENDING

Dariusz Rozumek

Faculty of Mechanical and Engineering, Technical University of Opole
e-mail: drozumek@po.opole.pl

The paper contains the results of experimental tests of the fatigue crack growth rate of steels 10HNAP and 18G2A under bending for different load ratios. In the tests, plane specimens with external unilateral sharp notches as stress concentrators were used. The results of the experimental tests are described by a nonlinear formula based on the ΔJ-integral range. The proposed formula for description of the fatigue crack growth rate, including the ΔJ-integral range, satisfactorily describes the results obtained experimentally.

Key words: fatigue crack growth, ΔJ-integral range, number of cycles, load ratio

Notations

a	–	length of the crack
l	–	length of the specimen
g	–	thickness of the specimen
c	–	length of the actual specimen section before the crack front
da/dN	–	fatigue crack growth rate
N	–	actual (propagating) number of cycles
ΔJ	–	integral range
R	–	load ratio
M_a	–	amplitude of the moment
B	–	coefficient in the equation
n	–	exponent in the equation
J_{Ic}	–	critical value of the integral
K_t	–	stress concentration factor

σ_u – ultimate tensile stress
σ_y – yield stress
ε_y – strain corresponding to the yield point
α_1 – material constant in the Ramberg-Osgood law
n_1 – exponent in the Ramberg-Osgood law
E – elastic modulus
ν – Poisson's ratio
K' – coefficient of strain cyclic hardening
n' – exponent of strain cyclic hardening

1. Introduction

Investigations of the fatigue crack growth rate and fatigue life constitute very important and complex problems in mechanics (Kocańda and Szala, 1997; Macha *et al.*, 2000). Application of the stress intensity factor K or its range ΔK for description of the stress field before the crack front in elastic-plastic materials is burdened with many errors caused by occuring large plastic strains. The coefficient K provides good results in the range of linear crack mechanics (Gasiak and Rozumek, 2001). For description of elastic-plastic and plastic materials, the criterion based on the J-integral, defined by Rice (1968), is suggested. This criterion describes an energy state in the crack front area. The Dowling and Begley (1976) linear model is widely used for description of the ΔJ-integral range. In the paper, authors compared the results obtained on the basis of their theoretical model with the experimental results. The agreement between these results was very good in the case of deflection control during the fatigue process. In the case of load control, significant differences were observed. The authors drew a conclusion that the proposed model did not give satisfactory results, and it was necessary to search for a more general criterion. Since there were many questions connected with the application of the J-integral for description of fatigue test results, Tanaka (1983) engaged in the research on that problem. He formulated an energy criterion based on the J-integral for the linearly-elastic and elastic-plastic ranges and its physical interpretation. Tests of the fatigue crack growth were performed for five materials (aluminium, copper, nickel, titanium and steel) under tension. Plane specimens with central slots were tested. It has been shown that for small strains and in the linear-elastic range, the J-integral can be determined independently of loading, as in the case of the monotonic J-integral. In the case of large strains in the elastic-plastic range, the cyclic J-integral depends on loading. However, in both cases, the cyclic J-integral remains constant while

loading (loading, unloading) if the first monotonic loading stage is eliminated. From the performed tests and considerations it results that the energy criterion based on the J-integral can be used under the fatigue crack growth.

The aim of this paper is the experimental verification of the proposed relationship for description of the fatigue crack growth rate and fatigue life in the energetic approach with the ΔJ-integral range.

2. Mathematical model

The paper presents an empirical formula for description of the second and third ranges of the crack kinetics curve (Rozumek, 2002) including the ΔJ-integral range

$$\frac{da}{dN} = \frac{B\left(\frac{\Delta J}{J_0}\right)^n}{(1-R)^2 J_{Ic} - \Delta J} \tag{2.1}$$

where $J_0 = 1\,\mathrm{MPa{\cdot}m}$ is a per unit value introduced to simplify the coefficient unit B.

In Eq. (2.1), the ΔJ integral range is calculated according to the finite element method

$$\Delta J = J_{max} - J_{min} \qquad J_{max(min)} = J_e + J_p = \frac{K^2}{E} + \frac{2Ap}{gc}$$

where the J_e integral concerns the linear-elastic period, and the J_p integral concerns the elastic-plastic period, $K = \sigma\sqrt{\pi a}$ is the stress intensity factor, A_p – area under the force-displacement curve, and from relationship (2.2)

$$\Delta J = \pi\left(M_k^2 \frac{\Delta\sigma^2}{E} + 1.13\Delta\sigma\Delta\varepsilon_p\sqrt{n'}\right)a \tag{2.2}$$

where: M_k is the correction coefficient including finity of the specimen dimensions (Pickard, 1986), $\Delta\sigma$ – stress range at the root of the notch, Δp – plastic strain range there.

Formula (2.1) allows one to calculate the number of propagation cycles N for which the crack reaches the critical value or the required value. The equation is then integrated from an assumed or found initial length of the crack a_0 up to the critical length a_f

$$N = \int_{a_0}^{a_f} \frac{(1-R)^2 J_c - \Delta J}{B(\Delta J)^n}\, da \tag{2.3}$$

After integration of Eq. (2.3), we obtain

$$N = B^{-1}\Big[\frac{\pi\Delta\sigma_a^2}{E} + \alpha_1\Delta\sigma_y\Delta\varepsilon_y\Big(\frac{P_a}{P_0}\Big)^{n_1+1}h_1\Big]^{-1}\cdot$$
$$\cdot\Big\{\frac{(1-R)^2J_c}{n-1}\Big[\frac{1}{(\Delta J_0)^{n-1}} - \frac{1}{(\Delta J_f)^{n-1}}\Big] - \frac{1}{n-2}\Big[\frac{1}{(\Delta J_0)^{n-2}} - \frac{1}{(\Delta J_f)^{n-2}}\Big]\Big\} \tag{2.4}$$

where ΔJ_f is the range of J_f corresponding to material failure, ΔJ_0 concerns the initial crack length a_0, P_0 is the limit loading ($P_0 = 0.536\sigma_y c^2 g/l$), h_1 – tabulated function specific for a given material and geometrical parameters of the specimen (Neimitz, 1998). The equation is valid for $n \neq 1$ and $n \neq 2$. If it is difficult to calculate the ΔJ-integral range and correction coefficients, we can use numerical methods

$$N = \int_{a_0}^{a_f} \frac{(1-R)^2J_c - \Delta J}{B(\Delta J)^n}\,da \approx \sum_{a_0}^{a_f} \frac{(1-R)^2J_c - \Delta J}{B(\Delta J)^n}\,\Delta a \tag{2.5}$$

3. Materials and test procedure

The subject of the investigations are construction steels 10HNAP and 18G2A characterised in Polish Standards, which concern low-alloyed and corrosion-resisting steels. Weldable steel 10HNAP is of general purpose and exhibits increased resistance to atmospheric corrosion. Steel 18G2A has improved mechanical properties. Their composition and properties are given in Table 1.

Table 1. Characteristics of 10HNAP and 18G2A steels

Steel	Chemical compositions [%]			Mechanical properties
10HNAP	0.14 C	0.88 Mn	0.31 Si	$\sigma_y = 418$ MPa, $\sigma_u = 566$ MPa,
	0.066 P	0.027 S	0.73 Cr	$E = 2.15 \cdot 10^5$ MPa, $\nu = 0.29$,
	0.30 Ni	0.345 Cu		$J_{Ic} = 0.178$ MPa·m
				(ASTM E813, 1989)
18G2A	0.20 C	1.49 Mn	0.33 Si	$\sigma_y = 357$ MPa, $\sigma_u = 535$ MPa,
	0.023 P	0.024 S	0.01 Cr	$E = 2.10 \cdot 10^5$ MPa, $\nu = 0.30$,
	0.01 Ni	0.035 Cu		$J_{Ic} = 0.331$ MPa·m

The parameters of the cyclic strain curve are as follows:

10HNAP steel:	$K' = 832\,\text{MPa}$,	$n' = 0.133$	(cyclic softening);
18G2A steel:	$K' = 869\,\text{MPa}$,	$n' = 0.287$	(cyclic hardening).

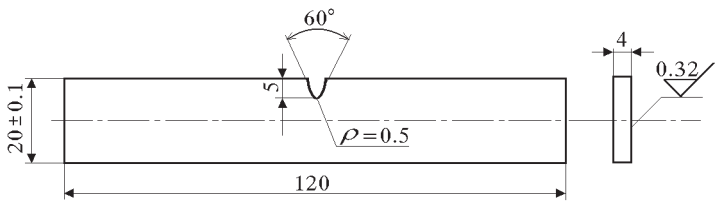

Fig. 1. Shape and dimensions of notched specimen

The tested specimens were cut out from a of 10 mm thick plate in the rolling direction. Figure 1 shows the dimensions and shape of the specimen. The specimens had an external, unilateral notch which was 5 mm deep and $\rho = 0.5$ mm in radius. The notches were made by milling, and the surface of the specimens was ground. The theoretical stress concentration factor in the specimen under bending, $K_t = 3.27$, was estimated with use of the model by Thum *et al.* (1960). The tests were done on the fatigue test stand MZGS-100 (Achtelik and Jamroz, 1982), enabling realisation of cyclic loading with a mean value inducing the plane stress on the material surface. The propagating crack length was measured by an optical device including a digital micrometer and a microscopic telescope magnifying 25 times. The fatigue crack length was periodically measured after some thousands of cycles, with an accuracy not less than 0.01 mm. Unilaterally restrained specimens were subjected to cyclic bending moment of the amplitude $M_a = 15.64\,\text{N·m}$.

3.1. Numerical method

The ΔJ-integral range, i.e. values of J_{max} and J_{min}, was numerically determined by the finite element method (FEM). For this purpose, the program FRANC2D was applied. It allows one to calculate the energy dissipated during the fatigue crack growth in an elastic-plastic material. The program includes nonlinear physical relationships obtained from the cyclic stress-strain curve of the materials tested. In this case, the cyclic strain curves for steels 10HNAP and 18G2A described by the Ramberg-Osgood relation were used. Calculations were done in an incremental way for flat notched specimens (Fig. 1) loaded in a cyclic manner by a bending moment of the constant mean value M_m and amplitude M_a.

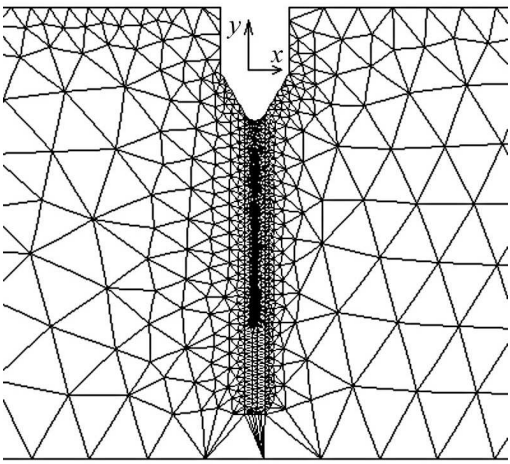

Fig. 2. Finite element mesh in the notched area

In the place of the notch, the fatigue crack (according to observations) was initiated, which propagated along the cross section of the specimen. Figure 2 shows a division of the area around the crack into finite elements. In the modelling, 6-nodal triangular finite elements were used; the triangles were of different dimensions. Calculations were done under the same loadings as those applied during the tests.

4. Experimental results

The paper contains test results which allow one to show phenomena occurring in 10HNAP and 18G2A steels during the fatigue crack growth process under bending for different load ratios R. The tests were performed under controlled loading from the threshold value to the specimen failure. The experimental results were presented as graphs of the crack growth rate da/dN versus ΔJ-integral range. Fig. 3 and Fig. 4 present graphs of the fatigue crack growth rates versus ΔJ-integral range for two kinds of materials, three load ratios under constant loading, calculated with the finite element method and Eqs (2.1) and (2.2). It has been observed that in 10HNAP and 18G2A steels the stress ratio changes from -1 to 0 as the fatigue crack rate increases, see Fig. 3 and Fig. 4 (graphs 1,2,3). From a comparison of the test results for 10HNAP and 18G2A steels it appears that a slower rate of the increase

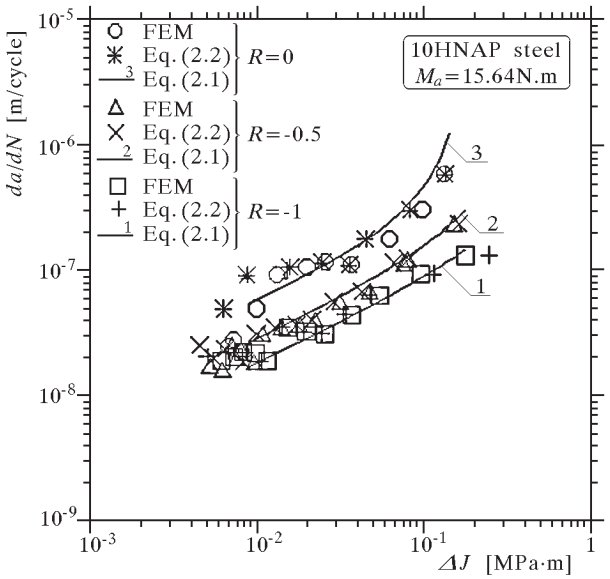

Fig. 3. Comparison of results found from FEM and Eqs (2.1) and (2.2) for 10HNAP steel

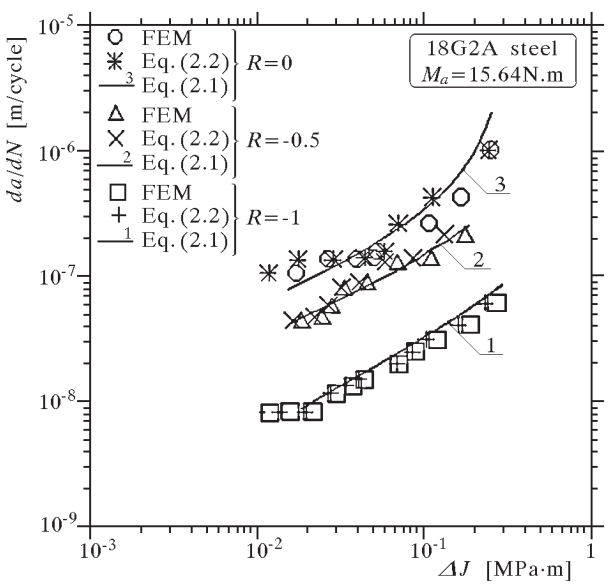

Fig. 4. Comparison of results found from FEM and Eqs (2.1) and (2.2) for 18G2A steel

of the fatigue crack growth is observed in the specimens of 10HNAP steel for $R = -0.5$ and 0. In formula (2.1) the coefficient B and exponent n for 10HNAP steel are $B = 3.0 \cdot 10^{-7}$ MPa·m^2/cycle and $n = 0.63$, respectively. For 18G2A steel they are $B = 3.5 \cdot 10^{-7}$ MPa·m^2/cycle and $n = 0.62$. The coefficients B and n, which should be material constants, are in practice dependent on other factors, for example the stress ratio R. In the presented tests, a relative error for the exponent n did not exceed 20%, and in the case of B it varied within $\pm 20\%$. As for 10HNAP steel, the maximum relative error was 17% (Fig. 3) under correlation at the significance level $\alpha = 0.05$, $r = 0.98$ for $R = -1$, $r = 0.96$ for $R = 0.5$ and $r = 0.91$ for $R = 0$. For 18G2A steel the maximum relative error did not exceed 14% (Fig. 4) under correlation $r = 0.98$ for $R = -1$, $r = 0.99$ for $R = -0.5$ and $r = 0.98$ for $R = 0$. The correlation coefficients assume large values in all considered cases which means that there is significant correlation between the test results and the assumed relationship, see Eq. (2.1). The coefficient B and the exponent n were determined with the help of the least square method. From a comparison of the results obtained by making use of the finite element method and those found analytically from Eq. (2.2), it appears that the difference between the obtained results is less than 10%.

From the analysis of experimental results (Fig. 3 and Fig. 4) for 10HNAP and 18G2A steels with different load ratios it appears that formula (2.1) describes the fatigue crack growth rates in the considered materials and loadings in a satisfactory way. Thus, it is possible to consider its applicability to the prediction of the fatigue life according to Eq. (2.4). In this equation, the parameters from the Ramberg-Osgood equation are: $\alpha_1 = 10.74$ and $n_1 = 2.26$ for 10HNAP steel and $\alpha_1 = 15.98$ and $n_1 = 2.60$ for 18G2A (necessary for calculation of the J_{p1}-integral according to Neimitz (1998)). The strength properties of the material and the critical values of the J_{Ic}-integral given in Table 1 were used in calculations. Having these data, the calculation life was determined for the results from FEM. The results of analyses were shown in the from of graphs comparing the calculation life N_{cal} with the experimental life N_{exp} (Rozumek, 2002).

In Fig. 5 and Fig. 6, the solid line means perfect agreement between the calculation and experimental lives, but the broken lines express the interval where the ratio of the calculation life to the experimental life is $N_{cal}/N_{exp} = 3$. Considering the calculation results obtained for load ratios $R = -1, -0.5, 0$ (Fig. 5 and Fig. 6), we can say that both considered steels show good agreement between the calculation and experimental lives in the scatter band $N_{cal}/N_{exp} = 3$. Thus, proposed nonlinear formula (2.1) can be applied to analysis of the consi-

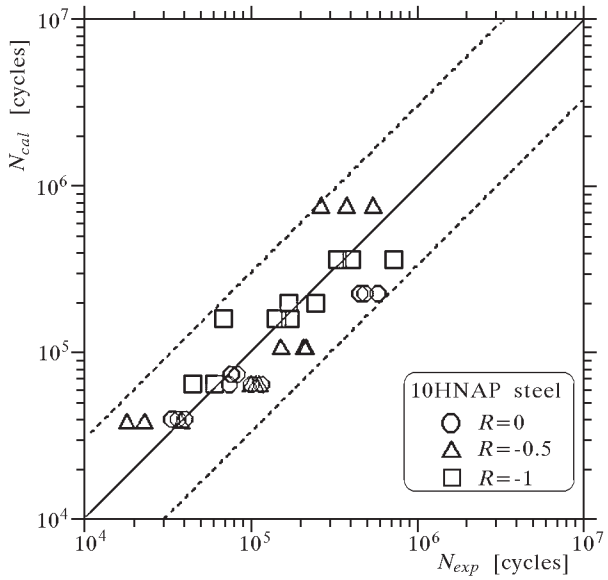

Fig. 5. Comparison of calculated and experimental fatigue lives for 10HNAP steel

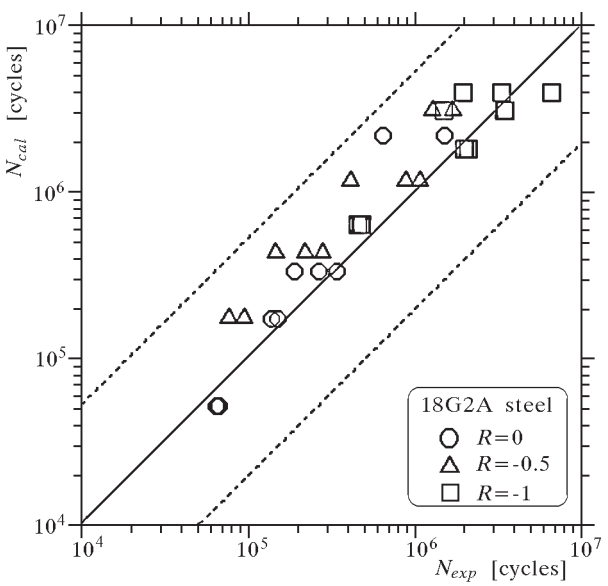

Fig. 6. Comparison of calculated and experimental fatigue lives for 18G2A steel

dered materials for determination of the fatigue crack growth rate and fatigue life in the propagation period.

5. Conclusion

The tests of fatigue crack propagation in plane notched specimens of 10HNAP and 18G2A steel subjected to cyclic bending show that for load ratios varying from -1 to 0 the fatigue crack rate increases together with a change in R. The fatigue crack growth rate causes drop in the number of cycles. Presented empirical formula (2.1) describes the test results well for both the crack growth rate and life. Comparison of the results found from the finite element method and Eq. (2.2) indicates only small differences – less than 10%.

Acknowledgements

This work was supported by the Commission of the European Communities under the FP5, GROWTH Programme, contract No. G1MA-CT-2002-04058 (CESTI).

References

1. ACHTELIK H., JAMROZ L., 1982, Patent PRL No. 112497, CSR No. 200236, HDR No. 136544, Warsaw (in Polish)
2. ASTM E813-89, 1989, Standard test method for J_{Ic}, a measure of fracture toughness, American Society for Testing and Materials, Philadelphia
3. DOWLING N.E., BEGLEY J.A., 1976, Fatigue crack growth during gross plasticity and the J-integral, *American Society for Testing and Materials*, ASTM STP 590, 82-103
4. GASIAK G., ROZUMEK D., 2001, Fatigue crack propagation in notched specimens under bending with the influence of mean stress, *Materials Technology*, **2**, 108-112 (in Polish)
5. KOCAŃDA S., SZALA J., 1997, *Basics of Fatigue Calculations*, PWN, Warsaw (in Polish)
6. MACHA E., PAWLICZEK R., ROZUMEK D., 2000, Fatigue tests of smooth and notched specimens under combined bending and torsion with influence of mean stress, *Materials Technology*, **2**, 79-85 (in Polish)

7. NEIMITZ A., 1998, *Fracture Mechancis*, PWN, Warsaw (in Polish)

8. PICKARD A.C., 1986, *The application of 3-dimensional finite element methods to fracture mechanics and fatigue life prediction*, London

9. RICE J.R., 1968, A path independent integral and the approximate analysis of strain concentration by notches and cracks, *Journal of Applied Mechanics*, **35**, 379-386

10. ROZUMEK D., 2002, Investigation of the influence of specimen geometry, concentrator type and kind of the material on fatigue life under cyclic bending, Doctoral Thesis, Technical University of Opole (in Polish)

11. TANAKA K., 1983, The cyclic J-integral as a criterion for fatigue crack growth, *Int. J. Fracture*, **22**, 91-104

12. THUM A., PETERSEN C., SWENSON O., 1960, *Verformung, Spannung und Kerbwirkung*, VDI, Duesseldorf

Wpływ obciążenia średniego na prędkość wzrostu pękania zmęczeniowego i trwałość przy zginaniu

Streszczenie

W pracy przedstawiono wyniki badań doświadczalnych wzrostu prędkości pęknięć zmęczeniowych przy zginaniu w stalach 10HNAP i 18G2A dla różnych wartości współczynnika asymetrii cyklu R. Do badań użyto próbek płaskich z koncentratorem naprężeń w postaci zewnętrznego jednostronnego karbu ostrego. Wyniki badań doświadczalnych opisano nieliniowym związkiem zawierającym zakres całki ΔJ. Zaproponowany związek do opisu prędkości rozwoju pęknięcia zmęczeniowego, zawierający zakres całki ΔJ, w sposób zadawalający opisuje wyniki uzyskane doświadczalnie.

Manuscript received July 7, 2003; accepted for print September 10, 2003